Extended norm-conserving pseudopotentials

Eric L. Shirley
Department of Physics and Materials Research Laboratory, University of Illinois, Urbana, Illinois 61801

Douglas C. Allan
Applied Processes Research, Corning Glass Works, Corning, New York 14831

Richard M. Martin
Department of Physics and Materials Research Laboratory, University of Illinois, Urbana, Illinois 61801

J. D. Joannopoulos
Department of Physics, Massachusetts Institute of Technology, Cambridge, Massachusetts 02139
(Received 15 March 1989)

Atomic pseudopotentials simplify electronic calculations by eliminating atomic core levels and the potentials that bind them. Outside some core radius, norm-conserving pseudopotentials produce the same scattering properties (radial logarithmic derivatives of wave functions for angular momenta of interest) as full-atomic potentials to zeroth and first order in energy about valence-level eigenvalues. We extend the correctness of the radial logarithmic derivative one order further in energy and present analytic and numerical results showing that this extension improves higher-order energy derivatives as well. We also show how our change improves predictions of excited single-particle eigenvalues in a wide variety of atoms, as well as high-energy scattering properties, with effects visible in a band-structure calculation. Our potentials converge nearly as quickly in reciprocal space as the Vanderbilt (modified Hamann-Schlüter-Chiang) potentials from which they are derived, and are easily generated.

I. INTRODUCTION

Determining the electronic structure of a physical system such as a solid is a difficult task, since the electrons form a many-body system of interacting fermions moving in the strong potentials of atomic nuclei. Calculating desired quantities such as binding and quasiparticle excitation energies can be extremely demanding when such quantities are a small fraction ($\sim 10^{-4}$–10^{-6}) of the system's total energy. The problem can often be greatly reduced, however, as the difficulties associated with such a calculation can largely be separated into two categories and confronted individually, namely the description of single-body and many-body aspects of the physical system.

Single-body aspects of a system relate to the accurate description of single electrons moving in some self-consistent field. Deep potentials in atomic cores lead to highly oscillatory wave functions difficult to describe in convenient basis sets, and the very number of electrons in a reasonably large atom makes the problem all the more hard. It has been demonstrated, however, that except for purposes of orthogonality to core wave functions due to the exclusion principle, it is not essential for correct valence properties of an atom that valence electrons experience a deep negative potential and exhibit highly oscillatory wave functions inside the core region.[1,2] Furthermore, deep core electrons can usually be treated as frozen in space and independent of an atom's valence environment (the frozen-core approximation), not only because of the disparity between valence- and core-level energy scales but also due to a variational theorem in density-functional theory.[3] With the above features of atoms in mind, *ab initio* ionic pseudopotentials[4] simplify the description of a physical system by removing altogether the atomic core levels and the potentials which bind them.[5] Deep full-atomic potentials are replaced by ones whose lowest bound states correspond to valence eigenvalues, and the resultant smooth pseudopotentials and nodeless valence wave functions can be accurately described using a variety of basis sets.

Many-body aspects of a physical system are important for even qualitatively correct solutions of electronic problems. One method which has been widely used to deal with many-body effects is the density-functional approach.[6] In particular, the local-density approximation[7] (LDA) reduces the description of a many-electron system to a set of local, self-consistent single-particle equations (the Kohn-Sham equations), simplifying the treatment of exchange/correlation effects by including such effects only approximately. Progress beyond local-density formulations of density-functional theory includes the application of Hedin's GW approximation[8] and quantum Monte Carlo techniques[9] to solids.

The above pseudopotential and many-body approximations used for describing physical systems can in principle be made and/or improved upon independently. Due to the sophistication of present pseudopotential techniques, most of the physical inaccuracy made in electronic structure calculations can be attributed to the inaccurate treatment of many-body effects rather than single-body effects. With current advances in many-body techniques, however, this situation could change. We shall focus here on improvements in norm-conserving pseudopoten-

tial (NCPP) techniques used in simplifying single-body aspects of the system within the context of the LDA, studying errors caused by using pseudopotentials by comparing different pseudopotential calculations to full-atomic ones but keeping the treatment of many-body effects unchanged.

Current NCPP's have the correct zeroth- and first-energy derivatives of a wave function's radial-logarithmic derivative at a valence eigenvalue; we extend this to be correct one order higher in energy, which simultaneously improves higher-energy derivatives as well. We first present analytic results on the energy dependence of the scattering properties of a central potential and the effects of external perturbations thereon, thereby providing some insight into the consequences of our extension. We then describe the implementation of our formal improvement, *extended norm conservation,* and demonstrate its effects in a wide variety of atoms. As a final test of our improvement, we present its effects on a band-structure calculation for silicon.

II. THEORETICAL BACKGROUND

In this section, we consider the single-particle, nonrelativistic Schrödinger equation for a spherically symmetric potential as is used in self-consistent calculations of atomic structure. The atomic calculations in this paper are actually done relativistically using the Klein-Gordon or Dirac equation, but Schrödinger's nonrelativistic equation leads to many formal relations relevant in our work. Since relativistic effects are small in the atoms we study, the formal relations which we derive here shall remain approximately true in our relativistic calculations. In Hartree atomic units, the radial form of Schrödinger's equation is

$$-\frac{1}{2}\frac{\partial^2}{\partial r^2}\phi(r)+\frac{l(l+1)}{2r^2}\phi(r)+[V(r)+\lambda U(r)]\phi(r) =E\phi(r)\ , \quad (1)$$

where the $\lambda U(r)$ term is included as a possible spherical perturbation on the potential $V(r)$, with $\lambda=1$ when the perturbation is at full strength. We can vary E about a single-electron valence eigenvalue and λ about zero to describe how the scattering properties of the atomic potential vary with energy and change under external perturbations.

We shall describe the scattering properties of $V(r)$ through the radial-logarithmic derivative of ϕ, i.e., ϕ'/ϕ, which we shall call x, and which is as informative as partial-wave scattering phase shifts.[10] We are using the phrase "scattering properties" in a loose sense, referring not so much to the problem of a positive energy electron incident on an atom as to the dependence of x on E and λ at any energy. Integrating the nonsingular solution of (1) from zero to a given atomic core radius R, one obtains some value of x at R. Bound states occur when this solution matches the decaying solution for $r>R$; scattering states occur for $E>0$.

Equation (1) can be written as a first-order nonlinear differential equation in x in the well-known form,

$$x'(r)+x(r)^2=2\left[V(r)+\lambda U(r)+\frac{l(l+1)}{2r^2}-E\right]\ . \quad (2)$$

Using the relation valid for any function $f(r)$,

$$f'(r)+2x(r)f(r)=\frac{1}{\phi(r)^2}\frac{d}{dr}[\phi(r)^2 f(r)]\ , \quad (3)$$

and differentiating (2) once with respect to E or λ, one obtains after multiplying by $\phi(r)^2$ and integrating,

$$\frac{\partial x(R)}{\partial E}=-\frac{2}{\phi(R)^2}\int_0^R dr\,\phi(r)^2 \quad (4)$$

and

$$\frac{\partial x(R)}{\partial \lambda}=+\frac{2}{\phi(R)^2}\int_0^R dr\,\phi(r)^2 U(r)\ , \quad (5)$$

which are valid for nodeless wave functions as well as for wave functions with nodes inside R. One can continue differentiation of (2) to get the following relation valid to all higher orders in E and λ but only for nodeless wave functions, where the prime in the sums means that we do not include the cases $a=b=0$ and $a=A$ when $b=B$ simultaneously:

$$\left[\frac{\partial}{\partial E}\right]^A\left[\frac{\partial}{\partial \lambda}\right]^B x(R)\Bigg|_{A+B>1} =\frac{-1}{\phi(R)^2}\sum_{a=0}^{A}{\sum_{b=0}^{B}}'\begin{bmatrix}A\\a\end{bmatrix}\begin{bmatrix}B\\b\end{bmatrix}\int_0^R dr\,\phi(r)^2\left[\left[\frac{\partial}{\partial E}\right]^a\left[\frac{\partial}{\partial \lambda}\right]^b x(r)\right]\left[\left[\frac{\partial}{\partial E}\right]^{A-a}\left[\frac{\partial}{\partial \lambda}\right]^{B-b} x(r)\right]\ . \quad (6)$$

For example, the second and third energy derivatives of x are

$$\frac{\partial^2 x(R)}{\partial E^2}=-\frac{2}{\phi(R)^2}\int_0^R dr\,\phi(r)^2\left[\frac{\partial x(r)}{\partial E}\right]^2=-\frac{8}{\phi(R)^2}\int_0^R\frac{dr}{\phi(r)^2}\left[\int_0^r dr'\,\phi(r')^2\right]^2 \quad (7)$$

and

$$\frac{\partial^3 x(R)}{\partial E^3}=-\frac{6}{\phi(R)^2}\int_0^R dr\,\phi(r)^2\left[\left[\frac{\partial x(r)}{\partial E}\right]\left[\frac{\partial^2 x(r)}{\partial E^2}\right]\right]$$

$$=-\frac{96}{\phi(R)^2}\int_0^R\frac{dr}{\phi(r)^2}\left\{\left[\int_0^r dr'\,\phi(r')^2\right]\left[\int_0^r\frac{dr'}{\phi(r')^2}\left[\int_0^{r'} dr''\,\phi(r'')^2\right]^2\right]\right\}\ . \quad (8)$$

Equation (6) states that any second or higher derivative of x can be expressed as a sum of integrals of products of $\phi(r)^2$ times pairs of lower derivatives, and one can readily see [e.g., in (7) and (8)] the iterative hierarchical scheme needed to achieve analytic expressions for all derivatives. These equations can in principle also be generalized to be applicable for wave functions with nodes when taking second and higher derivatives. When integrating through a node, however, the integrand with factor $\phi(r)^{-2}$, which will always arise in second- or higher-order derivatives, must be integrated carefully since the $\phi(r)^{-2}$ is related to the derivative of a first-order pole located at the node, or else one could use a method by Aharonov and Au.[11]

The above relations (4)–(8) can provide insight into the effects of our modification to NCPP's. Let us now briefly review the properties of NCPP's: We define a *pseudopotential* as a potential equal to the full-atomic potential outside of R, but shallow and possibly l-dependent inside so that the lowest single-particle bound state for each angular momentum of interest has an eigenvalue equal to that of the corresponding atomic valence level. A pseudopotential, therefore, eliminates atomic core levels and simplifies the description of valence levels. In a *norm-conserving pseudopotential,* the total charge inside R, divided by $\phi(R)^2$,

$$Q=\frac{1}{\phi(R)^2}\int_0^R dr\,\phi(r)^2 \tag{9}$$

is the same for the pseudo wave function as for the full-atomic wave function.

The correct matching of a valence orbital's Q by a pseudo wave function, termed *norm conservation,* assures that upon normalization a pseudo wave function will be equal to the full-atomic wave function outside of R rather than merely proportional to it. Within the (relatively minor) approximation of assuming a spherical charge distribution inside of the core radius, norm conservation also assures that the scalar potential generated by a pseudo wave function will be accurate outside of R. Equation (4), which was published originally by Lüders,[12] is pertinent in work relating to NCPP's because it demonstrates how Q and the first energy derivative of x will always be correctly matched at the same time. (The zeroth-energy derivative of x is already correctly matched at the valence eigenvalue because the real and pseudo wave function are equal for $r>R$.)

We extend norm conservation one order in E about valence eigenvalues by matching a pseudopotential's $\partial^2 x/\partial E^2$ as well as x and $\partial x/\partial E$. While we explicitly match only one more energy derivative of x, higher derivatives should generally be improved as can be seen from the form of Eq. (6). In practice, $\phi(r)^2$ will weigh most heavily in (6) near R, where $\phi(r)^2$ is both largest, and correct in value (in practice, up through its third radial derivative) so that if all derivatives of x lower than a given one are correct at R, then also that derivative of x at R should be close to the correct value. Later, we shall present examples of the improved accuracy of $\partial^3 x/\partial E^3$ which we achieved by matching $\partial^2 x/\partial E^2$.

While the E dependence of x is improved in the atomic configuration in which we generate our pseudopotentials, the λ dependence of x remains essentially uncorrected except when $U(r)$ is both approximately constant inside R, and correct. Thus, although we are improving some errors in the description of single-body aspects of an NCPP/LDA calculation, we are by no means addressing all of the errors present in such a calculation, nor do we necessarily deal with the largest. Some important errors which we do not touch on here include linearization of the nonlinear core-valence exchange-correlation interaction, which has been dealt with by Louie, Froyen, and Cohen,[13] the incorrect description of the valence-valence direct Coulomb and overlap terms (which are particularly apt to be numerically incorrect because of the change in valence charge density due to the removal of nodes),[14] and the frozen-core approximation, which plays a relatively minor role for reasons discussed by von Barth and Gelatt.[3]

III. IMPLEMENTATION OF EXTENDED NORM CONSERVATION

We generated extended NCPP's building on a previous method by Hamann, Schlüter, and Chiang[5] as modified by Vanderbilt.[15] Potentials produced by this method converge rapidly in reciprocal space, which is useful for band-structure calculations with plane-wave basis sets since relatively few plane waves are needed to represent wave functions and potentials. An alternative pseudopotential generating scheme by Kerker[16] produces pseudopotentials essentially equivalent to those of Hamann *et al.*, except that they do not to converge as rapidly in reciprocal space for reasons explained in Vanderbilt's paper. We were able to generate extended NCPP's using Kerker's scheme equally well, but with the particular goal of plane-wave calculations in mind we concentrate here on the Vanderbilt approach.

We refer the reader to Vanderbilt's paper for a more complete description of his scheme, which he describes in three steps. Our modification is only in the last step. In the first two steps, one generates a preliminary pseudopotential which has a lowest bound state with the correct valence eigenvalue but which generally does not obey norm conservation. In the third step, one modifies this potential's lowest bound-state wave function $y_l(r)$ by mixing in an envelope function $f_3(r/r_l)$ inside R in order to achieve norm conservation (where r_l is called the "cutoff radius" for a given angular momentum and is about $R/2$), and one scales the wave function by an overall constant for normalization purposes. One then inverts the Schrödinger equation to produce the binding potential associated with the resultant wave function $\phi_l(r)$ given by

$$\phi_l(r)=\gamma_l y_l(r)[1+\delta_l f_3(r/r_l)]\ . \tag{10}$$

We generalized Vanderbilt's form of $f_3(r/r_l)$ to fit $\partial x/\partial E$ and match $\partial^2 x/\partial E^2$ simultaneously (i.e., achieve *extended norm conservation*). To retain rapid reciprocal-space convergence of our pseudopotential as is present in Vanderbilt's, we did not want to change $f_3(r/r_l)$ in an arbitrary manner, but found the following alternative form adequate for our purposes:

$$f_3(u)=(1-mpu^n)100^{-\sinh^2\{u/[1.5+(1-m)p]\}/\sinh^2(1)}\ . \tag{11}$$

Vanderbilt's form of the envelope function $f_3(r/r_l)$ is the $p=0$ case of Eq. (11),

$$f_3^V(u)=100^{-\sinh^2(u/1.5)/\sinh^2(1)} . \quad (12)$$

The parameters m and n controlled the manner in which varying the fitting parameter p altered the form of $f_3(r/r_l)$. We varied m between zero and one in order to alternatively change the scale of the radial extent of $f_3(r/r_l)$ ($m=0$), alter the shape of $f_3(r/r_l)$ particularly at large r/r_l ($m=1$), or perform some admixture of the two operations ($0<m<1$). Flexibility of m was useful for extending norm conservation in a wide variety of atoms (discussed in the following section) and also provided us with additional control of the extent of the potential in reciprocal space. When $m\neq 1$ and thus the exponent n is used, n should neither be 1 or 3, which would, respectively, produce a $1/r$ dependence of or cusp in the potential at the origin. On the other hand, a large value of n would prevent $f_3(r/r_l)$ from decaying rapidly outside of the cutoff radius r_l, while a small value would not qualitatively change much the shape of $f_3(r/r_l)$. The value $n=6$ worked well for our purposes in extending norm conservation.

By carrying out the last stage of Vanderbilt's scheme repeatedly for different values of p, once m and n have been chosen, we were able to find a value of p which caused the potential to have the correct $\partial^2 x/\partial E^2$. [We determined the energy derivatives of x by finite-difference methods, integrating Schrödinger's equation from zero to R at various values energy of over a small range, both in the full-atomic potential and pseudopotential. We also explicitly fitted $\partial x/\partial E$ rather than Q because of relativistic corrections to (4).] Not wanting to alter the form of $f_3(r/r_l)$ very much, a small value of p was desirable, and we usually found a solution with

$$|p|<0.5 . \quad (13)$$

We generated extended NCPP's with x, $\partial x/\partial E$, and $\partial^2 x/\partial E^2$ fitted as accurately as one would desire at the valence eigenvalues, though in considerably more time than that required to generate the original Vanderbilt pseudopotential (on the order of 5 to 10 times longer, which is still reasonably fast). In all cases tested (though not with all core radii tried) an extended NCPP was achieved. We note that it may be possible that the third- and higher-order energy derivatives of x could also be achieved in a pseudopotential with the additional computational effort, in the spirit of our extension here to the second derivative. Nonetheless, the general existence of a pseudopotential producing an arbitrary number of correct energy derivatives of x remains yet to be demonstrated, and the increasing nonlinearity of (6) for higher derivatives renders such a demonstration foreboding. In any case, Levinson's theorem sets limitations on the energy range over which x can be correct, as pointed out by Hamann, Schlüter, and Chiang.

IV. EFFECTS OF EXTENDING NORM CONSERVATION ON ATOMIC CALCULATIONS

Because extension of norm conservation deals primarily with the E dependence of x and not the λ dependence, its effects should be sought in observing the wave mechanics of a single electron moving in the same self-consistent field in which the pseudopotential has been generated, but at energies different from the fitted valence eigenvalue. We present results on how extending norm conservation improves a pseudopotential's predictions of eigenvalues of excited states in the same self-consistent field, and also plot some curves of x versus E in the case of the full-atomic, norm-conserving, and extended norm-conserving potentials. Most atomic tests in this section were performed using the Klein-Gordon equation and the Wigner[17] interpolation scheme in the LDA.

As a test case, we made a pseudopotential for the $2s$ level in a $Z=3$ Coulomb potential, treating the $1s$ level as a core state, and observed how well norm-conserving and extended norm-conserving pseudopotentials predicted the known eigenvalues of the $3s$, $4s$, $5s$, and $6s$ states in the same Coulomb potential. In Table I, we tabulate these results as well as the excited-state eigenvalues for all atoms tested in this way, giving the eigenvalues (when present) in the full-atomic potentials, and the NCPP and extended NCPP errors in the eigenvalues. We also present the errors in the NCPP's and extended NCPP's third energy derivatives of x, which extension of norm conservation should improve, for reasons discussed earlier. From Table I, it is clear that NCPP's already predict higher single-particle states very well, but that the extension of norm conservation substantially reduces the

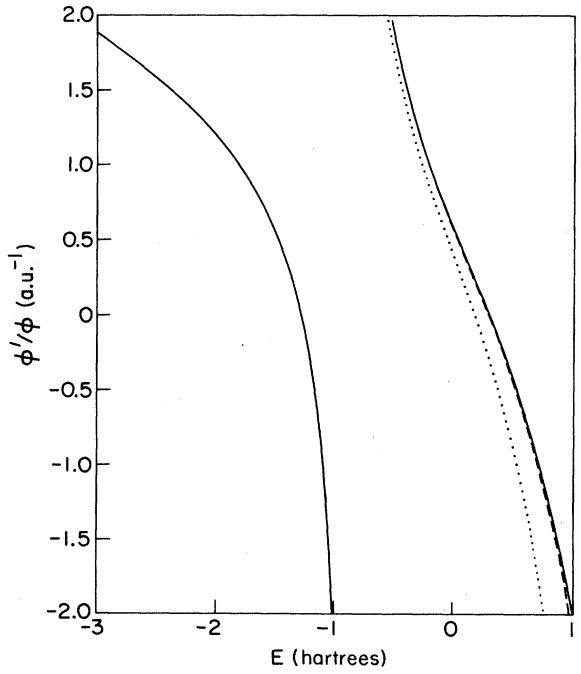

FIG. 1. Energy dependence of the radial logarithmic derivative in a $Z=3$ Coulomb potential. Displayed are the cases for the full potential (solid line), the Vanderbilt pseudopotential (dotted line), and our extended NCPP (dashed line). The discontinuity between -1.0 and 0.0 hartree occurs when a node passes through the sampling radius, 2.8 a.u. When a pseudopotential curve is not visible, it is superimposed on the full-potential curve.

TABLE I. (a) Excited one-electron level eigenvalues for a wide variety of atomic systems, in hartrees, as well as the errors produced by norm-conserving and extended norm-conserving potentials. (b) Core radii in atomic units and errors in third energy derivatives of x in hartree^{-3}, for the above systems.

(a)

System with pseudopotential		Excited one-electron level	Eigenvalue	Pseudopotential error NCPP	Pseudopotential error Extended NCPP
$Z=3$ Coulomb potential, $2s$ level		$3s$	−0.500 14	−0.003 94	−0.000 06
		$4s$	−0.281 31	−0.002 97	−0.000 06
		$5s$	−0.180 03	−0.001 89	−0.000 05
		$6s$	−0.125 02	−0.001 21	−0.000 03
C	$2s^1 2p^1$	$3s$	−0.438 28	−0.001 44	−0.000 23
		$3p$	−0.363 42	0.000 12	0.000 01
Si	$3s^2 3p^{0.5} 3d^{0.5}$	$4s$	−0.197 35	−0.000 72	−0.000 10
		$4p$	−0.137 22	−0.000 18	−0.000 02
		$4d$	−0.064 80	0.000 00	0.000 00
Mo	$5s^1 4d^{4.75} 5p^{0.25}$	$6s$	−0.011 24	−0.000 16	−0.000 02
Cu	$3s^2 3p^6 3d^9$	$4s$	−0.857 30	−0.014 78	−0.002 98
		$4p$	−0.570 78	−0.002 45	−0.000 05

(b)

System		r_l	Error in $\partial^3 x/\partial E^3$ NCPP	Error in $\partial^3 x/\partial E^3$ Extended NCPP
$Z=3$	s	1.4121	14.0992	0.0664
C	s	0.8	0.2920	0.0264
	p	0.6	−0.0184	−0.0024
Si	s	1.17	1.4232	0.1096
	p	1.35	1.5856	0.1288
	d	1.17	−0.1336	−0.0192
Mo	s	2.0	32.9400	2.0152
	p	2.0	3.1888	0.4384
	d	0.9	0.1048	0.0088
Cu	s	0.531	0.3712	0.0240
	p	0.545	0.1600	0.0072
	d	0.476	−0.0376	−0.0002

NCPP errors. In Fig. 1 the E dependence of x is plotted for the $Z=3$ full Coulomb, norm-conserving, and extended norm-conserving potentials. As should be expected, the extended NCPP curve is closer than the NCPP curve to the full-potential curve.

As a case where eigenvalues over a large energy range may be of interest, we included results for copper in Table I. We made a pseudopotential for the deep $3s$ and $3p$ electrons along with $3d$ electrons, rather than following the usual manner with $4s$ and $4p$ levels, treating closed $3s$ and $3p$ shells as core states. This results in having the lowest single-particle eigenvalues for each angular momentum of interest increase with increasing angular momentum, a condition necessary for using a pseudo-Hamiltonian developed by Bachelet, Ceperley, and Chioccetti.[18] Their pseudo-Hamiltonian is in turn generated from a norm-conserving potential such as Vanderbilt's or ours. The enormous difference in energy between the $3s$ and $4s$ levels (about 5 hartrees) led to a substantial error in the NCPP $4s$ eigenvalue (~ 0.5 eV) which is improved by our extension of norm conservation.

In Fig. 2 the E dependence of x in silicon is plotted for the pseudopotentials used in a solid-state calculation in the following section. We made the pseudopotential for silicon in the $s^2 p^{0.5} d^{0.5}$ configuration which was used by Vanderbilt to compare the reciprocal-space convergence of Hamann, Schlüter, and Chiang's potentials before and after his modification.[15] We present our silicon potentials and his in both direct and reciprocal space in Fig. 3. Ours are slightly more extended than Vanderbilt's in reciprocal space, but are comparable to those of Hamann, Schlüter, and Chiang as presented by Vanderbilt. (To invoke extended norm conservation in silicon, we used $m=0.75$, $n=6$.)

In Table II we present the excitation energies for atomic silicon in the all-electron NCPP and extended NCPP cases as a test of the interconfigurational transferrability

TABLE II. Excitation energies for atomic silicon. The energies are in hartrees and are relative to $s^2 p^2$. These were calculated using the Dirac equation and the Ceperley-Alder formula for exchange/correlation.

	$E(sp^3)$	$E(s^2 p)$	$E(s^2 p^{0.5} d^{0.5})$	$E(sp)$
All electron	0.2498	0.2878	0.4385	1.1748
Vanderbilt	0.2506	0.2882	0.4389	1.1752
This work	0.2504	0.2882	0.4388	1.1748

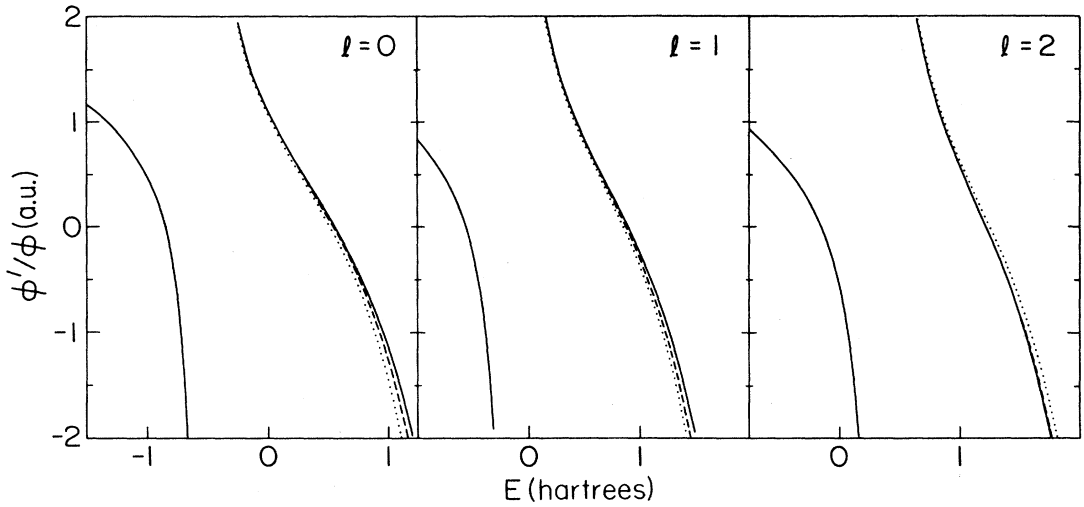

FIG. 2. Energy dependence of the radial logarithmic derivative in silicon for s, p, and d waves. Displayed are the cases for the full-atomic potential (solid line), the Vanderbilt pseudopotential (dotted line), our extended NCPP (dashed line). The discontinuities occur when a node passes through the sampling radius, 3.0 a.u. When a pseudopotential curve is not visible, it is superimposed on the full-potential curve.

of our pseudopotential. All of the atoms listed in Table I demonstrated our extended NCPP's to be comparable to Vanderbilt's potential in these regards, i.e., in terms of the accuracy of Kohn-Sham eigenvalue and total-energy shifts which occur upon changes of valence configuration. We point out, however, that inaccuracies in interconfigurational transferability relate mainly to the λ and not the E dependence of x, so we are not directly addressing such effects here.

V. EFFECTS OF EXTENDING NORM CONSERVATION ON BAND-STRUCTURE CALCULATIONS

A large number of complicating factors enter into the determination of the electronic structure of a solid from the atomic potentials once the appropriate NCPP's have been generated. Despite this, we have been able to observe the effects of our improvement on the atomic silicon pseudopotentials in the band structure of silicon. As discussed by Hamann, Schlüter, and Chiang[5] and in the spirit of Korringa-Kohn-Rostoker[19] (KKR) arguments, a pseudopotential's ability to accurately emulate the correct single-electron aspects of a band structure (such as band widths[20] and bonding-antibonding hybridization splittings[5]) depends on the energy range over which x is accurately predicted. A model problem showing how the energies of bands in a one-dimensional lattice are completely determined by the scattering properties of the constituent atoms is discussed by Heine.[2] In the case of a silicon lattice, the manner in which band energies are determined by the scattering properties of the atomic potentials is formally done using the KKR method.[21]

We determined silicon's band structure using a plane-wave basis set with Vanderbilt's NCPP and our extended NCPP generated in the $s^2p^{0.5}d^{0.5}$ configuration. We also carried out the calculations presented here with an NCPP and extended NCPP generated in the $s^1p^{0.5}d^{0.5}$ configuration and achieved results essentially identical to those presented here, except for a smaller[22] equilibrium lattice constant ($a=5.35$ Å). The potentials generated for the solid-state calculation were made using the full Dirac equation for atomic calculations and the Ceperley-Alder[23] formula for exchange/correlation as parametrized by Perdew and Zunger.[24] Desiring a highly converged comparison of the band structures produced using

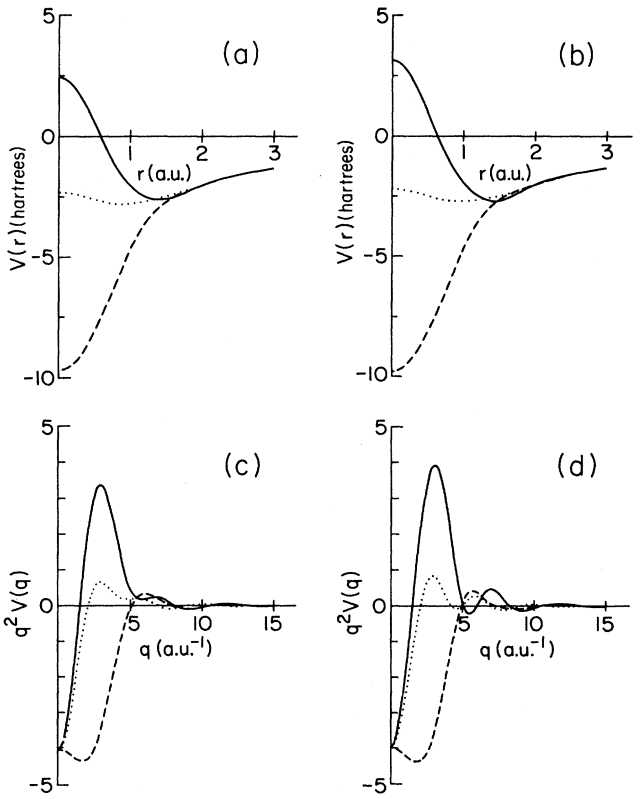

FIG. 3. Vanderbilt and extended NCPP pseudopotentials in direct and reciprocal space. Displayed are the potentials for $l=0$ (solid line), $l=1$ (dotted line), and $l=2$ (dashed line).

TABLE III. Pressure P at $a=5.43$ Å, the corresponding lattice constant based on the experimental bulk modulus $B=0.988\times10^{12}$ erg cm^{-3} and $a_{eq}\approx a[1+P(a)/3B]$, lattice constant and bulk modulus from an E_{tot} vs a curve, and the cohesive energy, calculated using the NCPP and extended NCPP for silicon, with experimental values for comparison. The overestimate of the theoretical cohesive energies is a systematic error because of the LDA. Atomic spin-polarization effects and zero-point energy, which we have not included in our calculation, are taken from Ref. 26.

	Potential		
	NCPP	Extended NCPP	Experiment
Pressure (kbar)	−30.821	−31.801	0.000
Lattice constant (Å)			
Based on pressure	5.376	5.374	5.429[a]
Based on minimum energy	5.373	5.377	5.429[a]
Cohesive energy (eV/atom)			
Spin-polarized atom, zero-point motion included	5.14	5.08	4.63[a]
Spin-unpolarized atom, zero-point motion ignored	6.00	5.94	
Bulk modulus (10^{12} erg/cm^{-3})	0.998	0.984	0.988[b]

[a]Reference 26.
[b]Reference 27.

the respective pseudopotentials, we used a 24 Ry (about 540 plane wave) cutoff and 10 special points.[25] Since (as is evident from Fig. 3) both Vanderbilt's and our potential are essentially converged after about 5 a.u.$^{-1}$, this calculation should be adequate to account for most features in the potentials.

From Fig. 2 we see that the NCPP and extended NCPP for silicon exhibit essentially identical scattering properties until energies well above the valence-level eigenvalues (-0.7452, -0.4712, and -0.1633 hartrees for $l=0,1,2$, respectively). Because all occupied bands in a self-consistent band-structure calculation are close to the atomic valence energies, values of physical quantities such as cohesive energy, equilibrium lattice constant, bulk modulus, and stresses should be similar using either a NCPP or extended NCPP. We see from Table III that the NCPP and extended NCPP are indeed equivalent regarding such quantities.

On the other hand, differences between a NCPP and extended NCPP should be visible when one deals with unoccupied states well above atomic valence levels, at which energies the pseudopotentials have noticeably different scattering properties. We note that high-energy bands are not superfluous in studying the physics of various systems. These bands are used, for example, in calculating the dielectric response of semiconductors[28] which is important for GW calculations,[8] and they are interesting in themselves because of many-body effects on their quasiparticle properties which have been observed experimentally.[29] The curves in Fig. 2 suggest that when using our extended NCPP to calculate such high-energy bands, those with atomic s- and p-like symmetry should be raised in energy, and d-like bands lowered, with respect to the corresponding bands derived from a NCPP calculation.

To examine the differences between the NCPP and extended NCPP band structures, we calculated the first 47 band energies at the zone center with both pseudopotentials. In diamond-structure silicon, Bloch functions at the zone center are either symmetric or antisymmetric about bond centers, and, if we choose the center of an atom as our origin, the Bloch functions then belong to representations[30] of the tetrahedral group T_d. s-like functions belong to the one-dimensional A_1 representation p_x-, p_y-, and p_z-, and d_{yz}-, d_{zx}-, and d_{xy}-like functions belong to the three-dimensional T_2 representation, and $d_{x^2-y^2}$- and $d_{3z^2-r^2}$-like functions belong to the two-dimensional E representation. Singly-degenerate bands (not counting spin degeneracies) can therefore be identified as exhibiting chiefly s symmetry, twofold degenerate bands can be identified as exhibiting chiefly d symmetry, and threefold degenerate bands have a mixture of p and d symmetry, in which case investigation of the wave functions near the center of the atom is required to determine which symmetry is dominant. f-like states and states of higher angular momentum are not important in bands in silicon until at very high energy, and we have ignored them.

Attempting to identify the dominant symmetries in the Bloch functions of the threefold degenerate bands, we Taylor-expanded their wave functions in real space about the center of the atom which we have chosen as our origin,

$$\Psi(\mathbf{r})=S+P_x x+P_y y+P_z z +D_{yz}yz+D_{zx}zx+D_{xy}xy+D_{x^2-y^2}(x^2-y^2) +D_{3z^2-r^2}(3z^2-r^2)+\cdots , \quad (14)$$

and formulated a criterion regarding the T_2 D and P coefficients to assign mostly p-like or mostly d-like atomic symmetry to the Bloch functions based on the ratio,

$$\alpha=\frac{|P_x|^2+|P_y|^2+|P_y|^2}{|D_{yz}|^2+|D_{zx}|^2+|D_{xy}|^2} . \quad (15)$$

By calling the four sets of threefold degenerate bands with the smallest α mostly d-like and the rest mostly p-like, the significant relative shifts of s-, p-, and d-like bands which occurred due to extending norm conserva-

TABLE IV. Zone-center band energies of the first 47 bands in diamond-structure silicon, the shift in energy due to extending norm conservation, and the assignment of the dominant atomic symmetry to the Bloch function based on the degree of degeneracy, or according to the criterion discussed in the text, for which cases we have given α as determined from the self-consistent calculation.

Degeneracy	α	NCPP band-energy (eV)	Shift (eV)	Symmetry
1		−11.981	0.043	*s*
3	1.0	0.000	0.000	*p*
3	0.88	2.621	−0.004	*p*
1		3.111	0.054	*s*
1		7.664	0.039	*s*
2		7.836	0.010	*d*
3	0.14	11.175	−0.001	*d*
1		15.080	0.029	*s*
3	0.007	22.947	0.015	*d*
2		24.116	0.006	*d*
3	0.57	25.127	0.242	*p*
3	0.008	29.438	0.006	*d*
3	0.0007	34.608	−0.034	*d*
1		37.394	0.510	*s*
2		38.420	−0.044	*d*
2		40.523	−0.055	*d*
3	3.4	41.349	0.387	*p*
3	164	43.879	0.113	*p*
1		44.248	0.361	*s*
3	0.81	44.950	0.076	*p*
3	0.55	45.209	0.009	*p*

tion can be said to have been predictable from the curves in Fig. 2, and we have equal numbers of sets of threefold degenerate T_2 mostly *d*-like bands and twofold degenerate E *d*-like bands. At high energies, the A_1 *s*-like bands have the largest positive shift, the E *d*-like bands have the largest negative shift, and the mixed *p*-like/*d*-like T_2 bands—understandably more ambiguous as to how extending norm conservation shifts them, due to their mixed symmetry—tend to shift more positively the more *p*-like they are.

In Table IV, we present our assignments of the atomic symmetries of the first 47 bands, as well as the band energies, degeneracies, and shifts in the band energies due to extending norm conservation. In Fig. 4 we plot as a function of energy the shift in band energy due to extending norm conservation for singly degenerate, doubly degenerate, triply degenerate mostly *p*-like, and triply degenerate mostly *d*-like bands. All band energies are taken relative to the valence-band edge. We conclude that the effects of extending norm conservation could be revelant in solid-state calculations. Presumably these effects are beneficial since, inasmuch as certain single-body aspects are concerned, extended NCPP's produce single-particle behavior closer to that of full-atomic potentials than do NCPP's.

VI. SUMMARY AND CONCLUSIONS

We have generated extended norm-conserving pseudopotentials and demonstrated improvements in the description of single-body aspects of atomic and solid-state applications due to our modification. Generally, the corrections achieved by extending norm conservation one order in energy will be small, and are not comparable to other errors in present calculational techniques. Nonetheless, they are unambiguous corrections to the description of certain single-body aspects of physical systems.

Our potentials are generated without much difficulty,

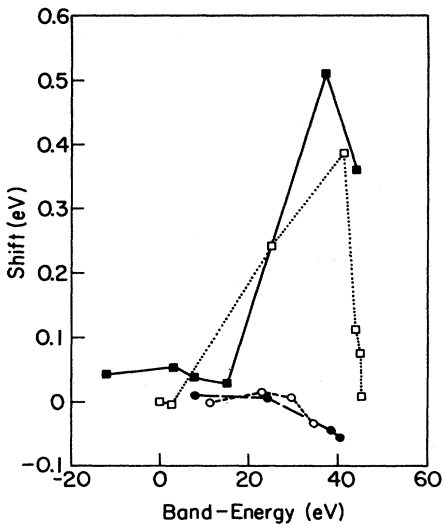

FIG. 4. Shifts in band energies due to extending norm conservation, as a function of band energy for singly degenerate (filled squares, solid line), doubly degenerate (filled circles, large dash line), triply degenerate mostly *p*-like (hollow square, dotted line), and threefold-degenerate mostly *d*-like (hollow circle, small dash line) bands. The lines are included to guide the eye.

though at the expense of being slightly harder than those previously developed. From the analytic viewpoint, our modification should present very few adverse side effects, but usually some dividends, such as the improvement of some terms of higher order than those which we explicitly correct. Nonetheless, because the equations defining the properties of extended norm conservation are nonlinear and have not been solved, we cannot guarantee the existence of an extended norm-conserving pseudopotential for all atomic systems and core radii.

Note added in proof. O. K. Andersen has pointed out that linearized band-structure methods [see, e.g., O. K. Andersen, Phys. Rev. B **12**, 3060 (1975) and H. L. Skriver, *The LMTO Method* (Springer, Berlin, 1984)] have scattering properties correct to 1 order higher in energy differences than in our scheme, but this requires retaining full atomic potentials and the accompanying core states.

ACKNOWLEDGMENTS

The pseudopotentials used in the solid-state calculation were generated using a modified version of the atomic program written originally by Sverre Froyen at the University of California at Berkeley, and the band-structure calculation was carried out on an FPS-164 array processor at the Materials Research Laboratory Computer Center using software written at the Xerox Palo Alto Research Center by K. Kunc, O. H. Nielsen, and R. J. Needs. We gratefully acknowledge assistance from Nithayanathan Chetty in using the programs. We benefited from discussions with G. K. Straub, G. Galli, Y. C. Chang, J. F. Annett, A. Muñoz, D. H. Vanderbilt, and others. This work was funded in part by the United States Department of Energy under Contract No. DE-AC02-76ER01198. Eric L. Shirley is supported by the Fannie and John Hertz Foundation.

[1]Morrel H. Cohen and V. Heine, Phys. Rev. **122**, 1821 (1961); B. J. Austin, V. Heine, and L. J. Sham, *ibid.* **127**, 276 (1962).

[2]Volker Heine, *Solid State Physics,* edited by H. Ehrenreich, F. Seitz, and D. Turnbull (Academic, New York, 1970), Vol. 24, p. 32.

[3]U. von Barth and C. D. Gelatt, Phys. Rev. B **21**, 2222 (1980).

[4]For a recent review, see Warren E. Pickett, Comput. Phys. Rep. **9**, 115 (1989).

[5]D. R. Hamann, M. Schlüter, and C. Chiang, Phys. Rev. Lett. **43**, 1494 (1979); G. B. Bachelet, D. R. Hamann, and M. Schlüter, Phys. Rev. B **26**, 4199 (1982).

[6]P. Hohenberg and W. Kohn, Phys. Rev. **136**, 864 (1964).

[7]W. Kohn and L. J. Sham, Phys. Rev. **140**, 1133 (1965).

[8]Lars Hedin and Stig Lundqvist, Solid State Phys. **23**, 1 (1969); Mark S. Hybertsen and Steven G. Louie, Phys. Rev. B **34**, 5390 (1987); R. W. Godby, M. Schlüter, and L. J. Sham, *ibid.* **37**, 10 159 (1988).

[9]S. Fahy, X. W. Wang, and Steven G. Louie, Phys. Rev. Lett. **61**, 1631 (1988).

[10]See, for example, Leonard I. Schiff, *Quantum Mechanics,* 3rd. ed. (McGraw-Hill, New York, 1968), p. 121.

[11]Y. Aharonov and C. K. Au, Phys. Rev. Lett. **42**, 1582 (1979).

[12]Gerbhart Lüders, Z. Naturforsch. **10a**, 581 (1955).

[13]Steven G. Louie, Sverre Froyen, and Marvin L. Cohen, Phys. Rev. B **26**, 1738 (1982).

[14]D. M. Ceperley suggested it may be most appropriate to seek a pseudo-Coulomb interaction and pseudo-kinetic-energy operator within the core region (private communication).

[15]David Vanderbilt, Phys. Rev. B **32**, 8412 (1985).

[16]G. P. Kerker, J. Phys. C **13**, L189 (1980).

[17]For a good discussion of Wigner's approximation, see David Pines, *Elementary Excitations in Solids* (Benjamin/Cummings, Reading, MA, 1983), pp. 89ff.

[18]G. B. Bachelet, D. M. Ceperley, and M. Chioccetti, Phys. Rev. Lett. **62**, 2088 (1989).

[19]J. Korringa, Physica **13**, 392 (1947); W. Kohn and R. Rostoker, Phys. Rev. **94**, 1111 (1954).

[20]Galen K. Straub and Walter A. Harrison, Phys. Rev. B **31**, 7668 (1985).

[21]Arthur R. Williams, Phys. Rev. B **1**, 3417 (1970), and references therein.

[22]This difference in lattice constant is understandable, since in the doubly ionized configuration the electrons are more tightly bound to the cores and will tend to draw the crystal closer together.

[23]D. M. Ceperley and B. J. Alder, Phys. Rev. Lett. **45**, 566 (1980).

[24]J. Perdew and A. Zunger, Phys. Rev. B **23**, 5048 (1981).

[25]D. J. Chadi and Marvin L. Cohen, Phys. Rev. B **8**, 5747 (1973); Hendrik J. Monkhorst and James D. Pack, *ibid.* **13**, 5188 (1976).

[26]M. T. Lin and Marvin L. Cohen, Phys. Rev. B **26**, 5668 (1982).

[27]Walter A. Harrison, *Electronic Structure and the Properties of Solids* (Freeman, San Francisco, 1980).

[28]Stefano Baroni and Raffaele Resta, Phys. Rev. B **33**, 7017 (1986); Mark S. Hybertsen and Steven G. Louie, *ibid.* **35**, 5585 (1987).

[29]W. B. Jackson and J. W. Allen, Phys. Rev. B **37**, 4618 (1988), and references therein.

[30]We consistently use the same notation as in Michael Tinkham, *Group Theory and Quantum Mechanics* (McGraw-Hill, New York, 1964).